

Redox Cycling of Copper–Amyloid β 1–16 Peptide Complexes Is Highly Dependent on the Coordination Mode

Lidia G. Trujano-Ortiz, Felipe J. González, and Liliana Quintanar*

Departamento de Química, Centro de Investigación y de Estudios Avanzados (Cinvestav), Avenida Instituto Politécnico Nacional 2508, San Pedro Zacatenco, 07360 Ciudad de México, D.F., Mexico

Supporting Information

ABSTRACT: Copper (Cu)–amyloid β (A β) interactions play a role in the etiology of Alzheimer's disease. This work presents a spectroscopic and electrochemical study of two physiologically relevant A β –Cu^{II} complexes, as a function of pH and relative Cu–A β (1–16) concentrations. Our results reveal that these coordination modes display distinct redox behaviors and provide experimental evidence for the existence of an intermediate Cu^I species. A mechanism for the redox cycling of these complexes is proposed, providing further insight into the redox relevance of A β –Cu interactions.

Alzheimer's disease (AD) is the most common neurodegenerative disorder in the world. One of the hallmarks of AD is the presence of extracellular deposits of amyloid β (A β) peptides,¹ while a high concentration of metal ions such as copper (Cu), zinc (Zn), and iron (Fe) is found in senile plaques.² Moreover, the interaction of A β with redox-active metal ions such as Cu^{I/II} and Fe^{II/III} is proposed to play a key role in the production of reactive oxygen species (ROS) and neuronal damage.³ The potential role of metal–A β interactions in the etiology of AD has sparked numerous studies on the coordination chemistry of A β in the past decade.⁴ On the basis of these studies two different coordination modes that are relevant at physiological pH have been structurally characterized, namely, modes I and II (Figure 1A). Mode I predominates at low pH (\sim 6.7), whereas increasing the pH (\sim 8.2) favors the formation of mode II. The coordination sphere for mode I involves two His residues at positions 6 and 13 or 14, the N-terminal group and an oxygen-based ligand. Mode II involves a deprotonated amide group (N[−]) that replaces one of the His ligands, while the oxygen-based ligand is assigned to the backbone carbonyl group of Ala2.⁵

The changes in the coordination sphere of Cu^{II} associated with the conversion of mode I to mode II would imply changes in the redox properties of the Cu–A β complex, yet information about how the redox potential of the Cu–A β complexes changes as a function of pH is still lacking. This study presents a spectroscopic and electrochemical characterization of Cu–A β complexes as a function of the pH. We find that these two coordination modes display distinct redox behaviors that reflect the different nature of their coordination spheres.

A titration of A β (1–16) with Cu^{II} at pH 7.5, followed by electronic absorption, circular dichroism (CD), and electron paramagnetic resonance (EPR) shows the presence of two

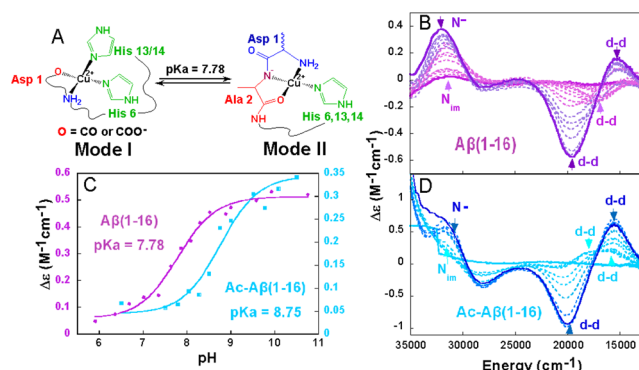


Figure 1. Structural models for Cu^{II}–A β (1–16) complexes at physiological pH (A). pH titrations of the Cu^{II} complexes with A β (1–16) (B) and Ac–A β (1–16) (D) at 0.5 mM with 0.7 equiv of Cu in 100 mM NEM with 100 mM NaCl, as followed by CD: pH 6.0 (light-blue lines) to pH 10.5 (dark-blue lines). pK_a values associated with CD changes at 31000 cm^{−1} for Cu–A β (1–16) (purple) and Cu–Ac–A β (1–16) (light blue) (C).

distinct species that correspond to coordination modes I and II (Figures S1 and S2 in the Supporting Information, SI). Our results indicate that the relative proportion of modes I and II is highly dependent on the Cu to A β (1–16) ratio. Upon the addition of a second Cu equivalent, modification of the EPR spectrum is in line with an increase of the mode II concentration (Figure S2 in the SI), consistent with an earlier study.⁶

Titration of the A β (1–16)–Cu^{II} complex by the pH, followed by CD (Figure 1B) and EPR (Figure S3A in the SI) shows that deprotonation drives the conversion of mode I, with a negative ligand-field signal at 17300 cm^{−1} and EPR parameters $g_z = 2.27$ and $A_z = 180 \times 10^{-4}$ cm^{−1}, into mode II, with $g_z = 2.23$ and $A_z = 157 \times 10^{-4}$ cm^{−1}, distinct d–d transitions at 15300 and 20000 cm^{−1}, and an intense ligand-to-metal charge-transfer (LMCT) band at 31900 cm^{−1} (313 nm), associated with an amide N[−]-to-Cu^{II} transition. A pK_a of 7.78 is associated with this conversion (Figure 1C), consistent with previous reports.⁷ A similar effect is observed for the acetylated form of the complex, Ac–A β (1–16)–Cu^{II}, because its CD and EPR features change drastically from pH 7 to 9.5, with a pK_a of 8.75 (Figures 1C,D and S3B in the SI). Namely, mode I' (with positive ligand-field transitions at 15600 and 17800 cm^{−1} and EPR parameters $g_z = 2.27$ and $A_z = 183 \times 10^{-4}$ cm^{−1}) turns into a species with distinct d–d

Received: August 15, 2014

Published: December 18, 2014

transitions at 15600 and 20000 cm^{-1} and an amide N^- -to- Cu^{II} LMCT band at 31600 cm^{-1} (316 nm), while the EPR spectrum indicates the presence of two different coordination modes (Figure S3B in the SI). Although the pK_a values and coordination models for the acetylated complex are different from those of the $\text{A}\beta(1-16)\text{-Cu}^{\text{II}}$ complex shown in Figure 1A (see Note 1 in the SI), their comparison is useful to interpret their electrochemical behavior, particularly because in both cases deprotonated amide groups participate in the coordination sphere of copper at pH values higher than their respective pK_a 's [7.78 for $\text{A}\beta(1-16)\text{-Cu}^{\text{II}}$ and 8.75 for the acetylated complex].

Figure 2A shows the cyclic voltammetry (CV) of the $\text{A}\beta(1-16)\text{-Cu}^{\text{II}}$ complex at different pH values, at a Cu to peptide ratio

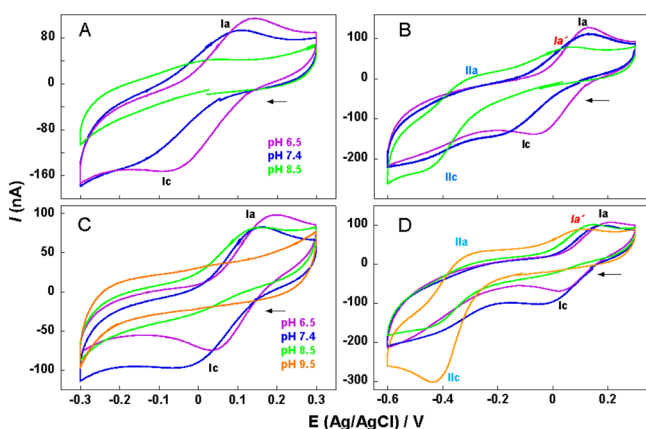


Figure 2. CV of $\text{Cu}^{\text{II}}\text{-A}\beta(1-16)$ (A and B) and $\text{Cu}^{\text{II}}\text{-Ac-A}\beta(1-16)$ (C and D) complexes at different pH values and potential ranges. The peptide concentration was 0.4 mM with 0.1 mM Cu^{II} in 10 mM phosphate buffer with 50 mM Na_2SO_4 as the supporting electrolyte. Scan rate: 5 mV s^{-1} .

of 0.25:1. Under these conditions, coordination mode I is prevalent at pH 6.5, where a cathodic peak (Ic) is observed at a potential of approximately -0.076 V, associated with the reduction of the complex, and an anodic peak (Ia) is observed at $\approx +0.140$ V, associated with the oxidation of the complex. This quasi-reversible behavior with a large anodic-to-cathodic peak difference suggests slow electron-transfer kinetics. Still, a formal potential of 0.032 V vs Ag/AgCl (0.255 V vs normal hydrogen electrode, NHE) can be determined for this reaction. This value is consistent with previous reports ranging from 0.28 to 0.30 V vs NHE (Table S1 in the SI).⁸ At higher pH values, the current intensities associated with peaks Ic and Ia decrease, while no current is recorded at pH 8.5 (green trace in Figure 2A). CV recorded in a wider range of potential clearly shows the presence of new cathodic and anodic peaks at pH 8.5 (IIc and IIa; green trace in Figure 2B), where coordination mode II is prevalent. These peaks are significantly shifted to more negative potentials, compared to those associated with coordination mode I observed at lower pH values. The formal potential for coordination mode II is -0.376 V vs Ag/AgCl (-0.153 V vs NHE). Thus, the formal potential associated with the reduction and oxidation of the $\text{A}\beta(1-16)\text{-Cu}^{\text{II}}$ complex shifts to more negative values by ~ 400 mV upon conversion of mode I into mode II. Such a large shift is consistent with having an amide N^- as a ligand for Cu^{II} in mode II (Figure 1A), as observed in other Cu^{II} -peptide systems, such as Cu complexes in the octarepeat region of the human prion protein.⁹ Certainly, a negatively charged hard ligand, such as a deprotonated amide, would provide further stabilization of the

Cu^{II} redox state of the complex, thus lowering its reduction potential.

CV of the $\text{Ac-A}\beta(1-16)\text{-Cu}^{\text{II}}$ complex at different pH values with a Cu-peptide ratio of 0.25:1 shows a similar behavior, except the trend is shifted by approximately one pH unit because of the shift in the pK_a of the complex. At pH 7.4, coordination mode I' is prevalent, and the cathodic (Ic) and anodic (Ia) peaks are observed with an associated formal potential of 0.060 V vs Ag/AgCl (0.283 V vs NHE; Figure 2C). At higher pH values, the intensities of peaks Ic and Ia decrease, while no current is recorded at pH 9.5 (orange trace in Figure 2C), where coordination modes with deprotonated amide groups are prevalent (see Note 1 in the SI). CV recorded in a wider range (orange trace in Figure 2D) leads to the measurement of a formal potential of -0.353 V vs Ag/AgCl (-0.130 V vs NHE). Again, similar to that observed for $\text{Cu}^{\text{II}}\text{-A}\beta(1-16)$, a decrease of ~ 400 mV is observed upon an increase of the pH, with the concomitant introduction of a deprotonated amide group in the Cu^{II} coordination sphere.

It should be noted that this trend in the reduction potential has been predicted recently by a theoretical study.¹⁰ Alí-Torres et al. calculated the reduction potentials for models of coordination modes I and II. A potential of 0.28 V was calculated for mode I, while their prediction for the reduction potential of mode II is -0.37 to -0.81 V. The authors associate the large shift in the formal potential to the presence of a negatively charged equatorial ligand that stabilizes the Cu^{II} redox state. Moreover, it is important to consider that a Cu-N bond that arises from coordination to an amide N^- is a highly covalent bond, as demonstrated by electronic structure calculations of Cu^{II} -prion complexes.¹¹ Thus, our electrochemical results are consistent with the coordination models for $\text{Cu}^{\text{II}}\text{-A}\beta(1-16)$ shown in Figure 1A and with the theoretical predictions of Alí-Torres et al., while they also underscore the conclusion that a negatively charged hard ligand, such as a deprotonated amide group, would provide strong stabilization of the Cu^{II} redox state of the complex.

Figure 3 shows a scheme for the redox cycling of the two physiologically relevant coordination modes of $\text{A}\beta(1-16)\text{-Cu}^{\text{II}}$.

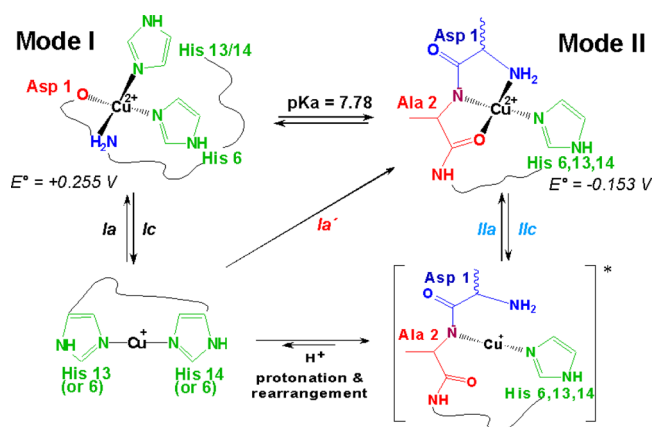


Figure 3. Mechanism for redox cycling of the $\text{Cu-A}\beta$ complex.¹³

The reduced form of this complex has been characterized only at $\text{pH} \approx 7$ by X-ray absorption spectroscopy and NMR, finding that Cu^{I} binds to two His residues in a linear fashion, preferentially using His13 and His14, although the presence of Cu^{I} complexes with combinations of His6 with His13 or His14 cannot be excluded.¹² The large structural changes associated with the

reduction of both coordination modes imply a large reorganization energy, explaining the observed quasi-reversible behavior and slow electron-transfer kinetics.¹³ In fact, in the cases where coordination mode II is prevalent (green trace in Figure 2B and orange trace in Figure 2D), the reoxidation process displays two anodic peaks: the most intense current is registered at peak IIa, associated with the reoxidation of mode II, while a small current is observed at peak Ia', a potential normally associated with reoxidation of mode I. This unusual behavior suggests the existence of two different forms of Cu^I complexes upon the reduction of mode II, which can be detected in our electrochemical experiment (Figure 3). Structural characterization of the reduced form of mode II has not been explored; however, recent computational studies have proposed transient structures that might serve as an intermediary during this reaction.^{4a,10,14} Namely, they find that, upon reduction of mode II, the first ligands to leave the coordination sphere are the N-terminal group and the backbone carbonyl, while a large geometric reorganization must happen to lead to a linear bis-His-Cu^I complex, involving protonation of the amide ligand and inclusion of a second His residue into the metal coordination shell (Figure 3). Although protonation reactions are fast, the geometric rearrangement for the His residue to coordinate Cu^I is predicted to be very slow,^{10,14} slow enough for our experiment to detect the reoxidation of such an intermediate Cu^I complex that readily converts into Cu^{II} coordination mode II at peak IIa, while the linear Cu^I species reoxidizes into Cu^{II} at peak Ia'. Indeed, the intensity of peak Ia' decreases drastically as the scan rate is increased (Figure S4 in the SI), reflecting significantly less accumulation of the rearranged linear Cu^I complex. Thus, our CV experiment provides direct experimental evidence for the existence of an intermediate Cu^I complex upon reduction of the A β (1–16)–Cu^{II} mode II.

In summary, our spectroscopic study reveals that the pH and relative Cu–A β ratio can modulate the population of coordination modes I and II. Electrochemical experiments show that these two A β (1–16)–Cu^{II} modes display very distinct redox behaviors. Considering the reduction potentials of physiologically relevant reducing agents, mode I would suffer reduction under physiological conditions, and thus it could activate oxygen for reduction and ROS production. In contrast, the reduction potential of mode II is very negative, so this species would not be reduced under physiological conditions. A β is present at the synapse, where there are transient changes in pH and copper concentrations.¹⁵ Thus, it is tempting to propose that the availability of the redox-inactive coordination mode II, which can be populated by an increase of the pH and/or Cu concentration, may be a protective mechanism to silence the redox activity of A β –Cu complexes. Interestingly, several naturally occurring N-terminal modifications of A β result in a lower pK_a for the conversion of mode I to mode II,¹⁶ and they may constitute a biological mechanism to silence the redox activity of A β –Cu complexes. Conversely, acidosis has been implicated in AD,¹⁷ and the low pH in the AD brain would favor the presence of the redox-active A β (1–16)–Cu^{II} mode I, potentially causing further oxidative damage.

■ ASSOCIATED CONTENT

■ Supporting Information

Experimental methodology, Figures S1–S4, and Table S1. This material is available free of charge via the Internet at <http://pubs.acs.org>.

■ AUTHOR INFORMATION

Corresponding Author

*E-mail: lilianaq@cinvestav.mx. Phone: +52-55-57473723.

Notes

The authors declare no competing financial interest.

■ ACKNOWLEDGMENTS

This research was funded by ICyTDF (Grant PIFUTP08-161) and CONACYT (Grants J48781Q and CB2009-128255 to L.Q. and a Ph.D. fellowship to L.G.T.-O.).

■ REFERENCES

- (1) Glenner, G. G.; Wong, C. W. *Biochem. Biophys. Res. Commun.* **1984**, *120*, 885–890.
- (2) Bush, A. I. *Trends Neurosci.* **2003**, *26*, 207–214.
- (3) Kozlowski, H.; et al. *Coord. Chem. Rev.* **2009**, *253*, 2665–2685.
- (4) (a) Faller, P.; et al. *Acc. Chem. Res.* **2014**, *47*, 2252–2259. (b) Karr, J. W.; et al. *J. Am. Chem. Soc.* **2004**, *126*, 13534–13538.
- (5) (a) Hureau, C. *Coord. Chem. Rev.* **2012**, *256*, 2164–2174. (b) Hureau, C.; Dorlet, P. *Coord. Chem. Rev.* **2012**, *256*, 2175–2187.
- (6) Alies, B.; et al. *Anal. Chem.* **2013**, *85*, 1501–1508.
- (7) Alies, B.; et al. *Inorg. Chem.* **2011**, *50*, 1192–11201.
- (8) (a) Bolland, V.; et al. *Proc. Natl. Acad. Sci. U.S.A.* **2010**, *107*, 17113–17118. (b) Jiang, D.; et al. *Biochemistry* **2007**, *46*, 9270–9282.
- (9) (a) Bonomo, R. P.; et al. *Chem.—Eur. J.* **2000**, *6*, 4195–4202. (b) Zhou, F.; Milhauser, G. L. *Coord. Chem. Rev.* **2012**, *256*, 2285–2296.
- (10) Ali-Torres, J.; et al. *J. Phys. Chem. B* **2014**, *118*, 4840–4850.
- (11) (a) Quintanar, L.; et al. *Coord. Chem. Rev.* **2013**, *257*, 429–444. (b) Rivillas-Acevedo, L.; et al. *Inorg. Chem.* **2011**, *50*, 1956–1972.
- (12) (a) Hureau, C.; et al. *J. Biol. Inorg. Chem.* **2009**, *14*, 995–1000. (b) Shearer, J.; et al. *Chem. Commun.* **2010**, *46*, 9137–9139. (c) Shearer, J.; Szalai, V. A. *J. Am. Chem. Soc.* **2008**, *130*, 17826–17835.
- (13) Note that a mechanism involving preorganized Cu^{II}/Cu^I structures for the processes Ia and Ic have been described in ref 8a.
- (14) Furlan, S.; et al. *J. Phys. Chem. B* **2012**, *116*, 11899–11910.
- (15) (a) Que, E. L.; et al. *Chem. Rev.* **2008**, *108*, 1517–1549. (b) Scheiber, I. F.; et al. *Prog. Neurobiol.* **2014**, *116*, 33–57.
- (16) Alies, B.; et al. *Inorg. Chem.* **2012**, *51*, 12988–13000.
- (17) Yates, C. M.; et al. *J. Neurochem.* **1990**, *55*, 1624–1630.